Digital Twin-enabled IoMT System for Surgical Simulation using rAC-GAN

Yonghang Tai, Liqiang Zhang, Qiong Li, Chunsheng Zhu, Victor Chang, Joel J. P. C. Rodrigues, *Fellow, IEEE,* Mohsen Guizani, *Fellow, IEEE*

***Abstract*— A digital twin-enabled Internet of Medical Things (IoMT) system for telemedical simulation is developed, systematically integrated with mixed reality (MR), 5G cloud computing, and a generative adversarial network (GAN) to achieve remote lung cancer implementation. Patient-specific data from 90 lung cancer with pulmonary embolism (PE)-positive patients, with 1372 lung cancer control groups, were gathered from Qujing and Dehong, and then transmitted and preprocessed using 5G. A novel robust auxiliary classifier generative adversarial network (rAC-GAN)-based intelligent network is employed to facilitate lung cancer with the PE prediction model. To improve the accuracy and immersion during remote surgical implementation, a real-time operating room perspective from the perception layer with a surgical navigation image is projected to the surgeon's helmet in the application layer using the digital twin-based MR guide clue with 5G. The accuracies of the area under the curve (AUC) of our new intelligent IoMT system were 0.92, and 0.93. Furthermore, the pathogenic features learned from our rAC-GAN model are highly consistent with the statistical epidemiological results. The proposed intelligent IoMT system generates significant performance improvement to process substantial clinical data at cloud centers and shows a novel framework for remote medical data transfer and deep learning analytics for digital twin-based surgical implementation.**

***Index Terms*—Digital Twin, IoMT, Remote Surgery, Robust Auxiliary Classifier Generative Adversarial Network (rAC-GAN) model, Mixed Reality**

I. INTRODUCTION

With the rise of artificial intelligence (AI), the Internet of Things (IoT), the digital twin (DT), and mixed reality (MR), it is well documented that the concepts of "smart medicine" and "precision medicine" have been tightly linked to these technologies thus far [1]. Combining multiple technologies to build a customized medical solution testbed for modern medicine has become a trend. Therefore, is it possible to bring together deep learning technologies, digital twins, mixed reality, and medical IoT technologies to create a medical IoT platform that can serve customized medical solutions? Subsequently, we develop a medical IoT platform based on clinical lung cancer combined with pulmonary embolism medical data already collected and combined with a rAC-GAN network to create a medical IoT platform with four technologies.

In China, the main difficulty in accessing medical care is not in the poor medical infrastructure, but in the fact that patients are looking for customized medical solutions from specialists. According to incomplete statistics, there are 24 tertiary hospitals in Yunnan, China, which has a resident population of more than 47 million people. As you can imagine, the popularity of such customized solutions is very difficult. It is noted in [2] that IoMT has been used to create medical experimentation platforms very commonly, often in combination with technologies such as display augmentation, mixed reality, and digital twins that are now mature. With the next 10 billion Internet of Things (IoT) devices coming online, we could see trillions of connected devices over the next year, and the earlier "50 billion devices" figure will still be widely cited in 2020 [3]. In such a context, it is proposed: to create a digital twin experimentation platform for customized medical solutions based on mixed reality and IoMT technologies to facilitate doctors' experiments with customized medical solutions and improve efficiency. By combining with the highly robust rAC-GAN deep learning network, we build a medical platform that is truly fast and efficient.

So, why do we use lung cancer combined with pulmonary embolism as our experimental data? On the

This work is supported by the Key-Area Research and Development Program of Guangdong Province (No. 2020B0101130006), the Major Key Project of PCL (PCL2021A15), and the National Key R&D Program of China (2020YFB2104301). This work was supported by grant funded by the National Natural Science Foundation of China (62062069, 62062070, and 62005235). This work is also partially funded by FCT/MCTES through national funds and when applicable co-funded EU funds under the Project UIDB/50008/2020; and by Brazilian National Council for Scientific and Technological Development - CNPq, via Grant No. 313036/2020-9. (*Corresponding authors: Qiong Li, Chunsheng Zhu, Victor Chang; Yonghang Tai and Liqiang Zhang contributed equally to this paper*)

Yonghang Tai is now with the Kunming University of Science and Technology, Kunming, China. He is also with the Yunnan Normal University, Kunming, Yunnan, China. (e-mail: taiyonghang@ynnu.edu.cn).

Liqiang Zhang, and Qiong Li are with the Yunnan Key Laboratory of Opto-electronic Information Technology, Yunnan Normal University, Kunming, Yunnan, China. (e-mail: lq394627@gmail.com, liqiong@ynnu.edu.cn).

Chunsheng Zhu is now with the Institute of Future Networks, Southern University of Science and Technology, Shenzhen, Guangdong, China. He is also with Peng Cheng Laboratory, Shenzhen, Guangdong, China. (e-mail: chunsheng.tom.zhu@gmail.com).

Victor Chang is now with the Aston Business School, Aston University, Birmingham, UK. (e-mail: victorchang.research@gmail.com).

Joel J. P. C. Rodrigues is now with the College of Computer Science and Technology, China University of Petroleum (East China), China. He is also with the Instituto de Telecomunicações, Portugal. (e-mail: joeljr@ieee.org).

Mohsen Guizani is now with the Machine Learning Department, Mohamed Bin Zayed University of Artificial Intelligence (MBZUAI), UAE. (e-mail: mguizani@ieee.org).

one hand, the geographical location of Yunnan, China, is unique in that it is home to a population with lung cancer combined with pulmonary embolism, which meets our goal of experimenting with customized medical solutions. On the other hand, the induction of malignancy is often associated l with venous thrombosis (VT) and pulmonary embolism (PE). In clinical studies, lung cancer is an important risk factor for PE [4], with a combined probability of approximately 3.7%. In the conventional approach, lung cancer combined with pulmonary embolism is determined according to the Chinese Society of Respiratory Medicine [5]. Therefore, the pathogenesis and risk factors for PE associated with lung cancer still need further study. Fortunately, several basic factors have been proposed that can be used to predict pulmonary embolism in combination with arterial blood gas analysis and X-ray [6]. However, patients rarely have time to listen to their physician's interpretation of their medical diagnosis [7]. Therefore, it is very important to implement a "digital twin". One of the most commonly used concepts is the concept of a "mediated translator". Currently, the traditional diagnostic processing of this mediated translator is known as pathological diagnosis, which leads to longer procedure times and increased operational risks. Therefore, algorithms from machine learning or deep learning [8][9] have the potential to assist oncologic surgeons in mining the deep relationship between surgical execution and medical data. However, predictive models developed in related studies were built on datasets lacking regional specificity [10]. Various results have shown that collinearity between variables is not easily resolved using regression models alone [11], which makes these results inapplicable to clinical decision-making. In our experiments, an interference-resistant rAC-GAN was used to classify and predict the collected data on lung cancer combined with pulmonary embolism and was further used to assist physicians in determining the correct symptoms of patients.

Internet of Medical Things (IoMT) technology has been successfully used in various research areas due to its utility and high performance [12]. Meanwhile, with the rise of the Industrial Internet, digital twins are gradually entering the public eye. In layman terms, a digital twin is a cloned digital version of a twin [13]. The rise of digital twins provides a better application platform for AI and IoT platforms. In the industrial world, each device in the physical world can have a virtual digital twin in the digital space. In the virtual world, the operational details of an actual device can be monitored in real time. Conversely, virtual devices can be manipulated to control real-world devices, indirectly enabling spatial and temporal breakthroughs. A digital twin combines various advanced technologies to create actual mapped devices in the virtual space, reflecting the relevant physical devices throughout the life cycle process. Continuous fine-tuning and optimization are performed to optimize the actual devices. Moreover, the health of the actual equipment can be monitored, analyzed, and processed through its digital twin. Thus, a digital twin enables many savings in terms of training costs for maintenance, repair, commissioning, and operation [14]. In the context of new drug development and patient surgery customization, clinical trials are characterized by high price, time and inefficiency. It is a great challenge to develop clinical trials because few patients meet the criteria and are willing to participate in the trials. Researchers can build experimental groups and construct digital twin models using data from completed experiments [15]. Then, we can implement a patient's customized medical regimen with the digital twin first and treat the patient after the regimen is successful. This improves the reliability and implementability of the protocol treatment.

It is pointed out in [16] that as industrial technology drives the continuous changes in IoT technology, digital twin technology will evolve exponentially with it. In [17], it is proposed that digital twin technology at the present stage is growing rapidly with IoT technology developing rapidly and continues to demonstrate its potential in various industries, while [18] suggests that digital twin technology combined with IoMT technology in the operating room has the potential to be used. However, at this stage, the use of these technologies is only in the collection of data and is less useful for medical diagnostic services. Based on this, we intend to build an experimental platform that can be used to experiment with physicians' customized medical solutions.

Due to deep learning which could enable accurate mapping of input features-output variables [19], a large number of deep learning techniques are used to fill in the missing data. [20] proposed a GAN network based on generating a larger number of samples to solve the problem of imbalanced data for a certain class of faulty samples. Anusha *et al* [21] proposed a KNN attribution-based technique due to the contribution of deep learning in target localization scenarios. It is used to fill the missing data and thus change the overall accuracy of target localization. However, the KNN attribution technique relies on the continuity of data, and most of the medical text data we have collected is discrete. Therefore, based on the above work on missing data filling, we propose a filling approach based on the DLI technique for filling the missing values of discrete clinical data.

IoMT technology has been continuously developed, and its connection with deep learning has become stronger and stronger. In [22], the feasibility of combining machine learning with IoMT networks was proposed, pointing out that some networks are not accurate and robust enough for data prediction. In [23], it was proposed to build a set of IoMT platforms using CNN networks for the diagnosis of lung cancer combined with pulmonary embolism, but with low robustness. So on the one hand, we chose the rAC-GAN algorithm so that the platform we built can better serve the physicians to experiment with customized medical solutions. On the other hand, we also want to be able to make our platform with high accuracy and robustness. rAC-GAN has high accuracy because the noise z present in the data is cleaned before the discriminator outputs the classification labels. It has high robustness due to its unique Nash equilibrium training method.

Our study aims to quantify and process data on lung cancer combined with pulmonary embolism in Yunnan and Chongqing provinces through a rAC-GAN model. Based on patient-specific data analysis and epidemiological analysis, 20 clinical features were summarized. Combining these features with digital twin technology, mixed reality and medical IoT technology, a medical platform for experimenting with customized medical surgical solutions is created. Four original contributions are summarized as follows:

1. The first interference-resistant rAC-GAN model for real-time outpatient data detection is proposed and implemented. The model was proven to be extremely resilient in the intelligent prediction of whether lung cancer is paired with pulmonary embolism in experiments.

2. To correct data imbalances, a deep learning-based imputation (DLI) data-population technique is used for medical data, followed by epidemiological statistics to assess the trustworthiness of the completed data.

3. An end-to-end framework based on the DLI data filling approach and the rAC-GAN model is proposed for pathology prediction on mixed data (containing redundant data) of patients with an accuracy of over 90%. We also use cost learning to improve detection accuracy while addressing data imbalance.

4. A novel remote surgical rehearsal platform based on reality augmentation technology was devised and deployed, combining the principles of predictive outcomes and digital twins to build an IoMT platform capable of completing customized medical service testing without injuring the human body.

The rest of the paper is organized as follows. Section II discusses the related work. Section III presents the system design. The evaluation results and further discussions are shown in Section IV and Section V, respectively. Section VI concludes this paper.

II. Related Work

A. AI-based Application for Medical Data

Experiments on medical data based on AI contain a large proportion of experiments on the lung. Akilandeswari *et al.* [24] researched case screening using AI for PE data processing. After comparison with four different types of defined frameworks, the experiment concluded that the CNN model based on inception has a good effect on detecting pulmonary embolism in lung CT scan images. Therefore, in this paper, clinical data on lung cancer combined with pulmonary embolism will be used to validate the accuracy of our network. At a time when there were minimal references between LC and PE, Li *et al.* [25] studied substantial material and concluded that there was a significant relationship between LC and PE. Wang *et al.* [26] investigated the associations of venous thrombus embolism in patients with newly diagnosed lung cancer and concluded that LC patients commonly have a high prevalence of venous thrombus embolism.

Machine learning-based traditional prediction models have been widely developed in clinical decision support for LC or PE patients, mainly because of their implementation combined with high reliability and interpretability. Li *et al.* [27] used a novel AI computer-aided diagnostic system to localize and quantitatively diagnose pulmonary embolism in CT angiography of the pulmonary arteries to verify the feasibility of AI-based intelligent diagnosis of pulmonary embolism. Similarly, an ML-based network model was designed to analyze longitudinal clinical indicators (the values of different clinical characteristics of patients) to generate a risk score for PE patients to predict the outcome of pulmonary embolism as clinical decision support for patients [28]. A total of 3214 clinical data points were included in that study, and the model had the best accuracy. In applying machine learning to such tasks, the algorithmic structure of random forests was used by Moll to extract important clinical features. Cox regression was also used to predict mortality, resulting in a mortality prediction model for chronic obstructive pulmonary disease with the highest accuracy [29]. Faced with an inadequate clinical dataset, Wang *et al.* proposed predicting the incidence of disease over the next year based on the available data and adopted machine learning to make predictions to confirm the validity of the generated data [30]. Sequential decision-making designed by Petousis *et al.* [31] is used to identify early-stage LC, in which multiple machine learning techniques are deployed to learn the decision process of partially observable Markov chain and then a dynamic Bayesian network as an observational model and inverse reinforcement learning is used to discover a reward function based on experts' decisions. The predictive results demonstrated that the proposed model can not only maintain a high accuracy on LC patients, which reaches the experts' level but also decrease the mistake diagnostic rate of the normal. Chen *et al.* [32] used machine learning to classify different pathological conditions of lung cancer patients. The experiments show that combining medical data and AI methods such as machine learning is an innovative, fast and convenient way to classify the corresponding pathologies. Liu *et al.* [33] improved the basic CNN network and proposed a DL-CNN model. This model has a higher AUC for quantitatively calculating the clot burden in patients with acute pulmonary embolism. Although rAC-GAN is not very widely used on medical data, it has demonstrated strong robustness and accuracy on the COVID-19 dataset in [11]. Therefore, we chose to apply the rAC-GAN network to the filled lung cancer with pulmonary embolism data. However, to the best of our knowledge, there is still a lack of research to study and develop a state-of-the-art model based on complicated clinical features. There is a demand to research and develop an advanced model with high reliability and interpretability.

B. The Evolution of the Internet of Medical Things

With the rapid development of IoMT technology in recent years, in 2017, Abawajy *et al.* responded to technological innovation and developed a pervasive patient health monitoring (PHM) system infrastructure by assembling IoT systems to meet the increasing service requirements of patients, fully reflecting the strong trend that the use of IoT technology in healthcare has now become a trend [34]. However, are AI algorithms (machine learning or deep

learning algorithms) helpful in terms of IoMT? In 2019, Durga *et al.* performed a survey on AI algorithms in IoT healthcare and found that algorithms such as machine learning and deep learning can improve the performance of IoMT systems and assist doctors in monitoring, diagnosing, and focusing on patients [35]. This demonstrates the feasibility of using deep learning in IoMT. In 2020, the teams of Tuli *et al.* [36] and Bibi *et al.* [37] published their latest research on IoMT. In [38], the authors combined machine learning algorithms with cloud computing to create a COVID-19 tracking and prediction system and successfully used the cloud to predict the growth of the pandemic accurately and in real-time. Authors in [39] successfully used deep learning algorithms combined with cloud computing to diagnose leukemia subtypes based on both DenseNet-121 and ResNet-34 frameworks. The research to date confirms the validity of using deep learning in IoMT technology, which in turn confirms that the use of deep learning algorithms in IoMT is an inevitable trend.

C. Digital Twin Implementations in Medical Simulation

Digital twinning has rich applications and broad prospects in product design, product manufacturing, medical analysis, engineering construction, and smart cities. Real-time is one of the characteristics of a digital twin. That is, a digital virtual entity can represent the real-time state of a physical entity with a changing time axis. Nondeterministic clock errors lead to degraded synchronization efficiency with increased network resource consumption. Focusing on IoT system synchronization problems, Jia *et al.* proposed a kind of clock synchronization scheme based on twin technology [40]. [41] mainly used a marginalized collaborative system architecture to build a digital twin model. The clock is simulated by gathering continuous information on the actual device to predict the time offset of each node. Healthcare has applications that have led to the rapid growth of wearable device-based intelligent application categories [42]. The popularity of wearable devices makes it more convenient to use sensors to obtain a human body and physiological data. When a large amount of data is collected by a sensor, we can analyze and model the data, judge the state of the user through the numerical value of various characteristics, and provide the user with more accurate and convenient services according to their state. For example, a numerical twin of the human body, such as a bracelet, could use vibrations to remind the user to relax when sitting for long periods. Anglo Croatti used digital twinning technology to realize the application of trauma management. This perspective makes it possible to explore the use of a DT's simulation features on the agent side to support agent decision-making [43]. In the course of cancer treatment, late diagnosis is a leading cause of medical complications. Liu *et al.* present a cloud-based IoT medical system framework based on digital twin health care. This is a new, generic, extensible framework for cloud environments for monitoring, diagnosing, and predicting health [44]. Using AI, visualization inside the human body has long been at the heart of medical imaging. Digital, physiological modeling of the human body is on the horizon. Using a digital twin as a customized computational model of a patient could provide a lifelong and personalized model and be continuously updated with new sensor data, scans, or exams. AI frameworks combined with the IoT can serve as a wellness coach (i.e., IoMT), predicting individual risks, and moving healthcare from treating sickness to coaching us on how to predict disease.

D. Mixed Reality Virtual Surgery

With the advancement of virtual simulation technology, virtual medical surgery training moves from two-dimensional to three-dimensional. Visualization systems using mixed reality technology also have strong applications in case discussion, surgical planning, and intraoperative guidance [45]. In 2016, Hamacher *et al.* [46] discussed the application of virtual reality (VR) and mixed reality (MR) technology based on their application to urology. It was pointed out that medical treatments based on VR and MR technologies will see rapid developments. By 2020, Verhey *et al.* [47] studied and realized the application of MR technology in orthopedic simulation surgery. Three-dimensional reconstruction of a patient's imaging was achieved without fluoroscopy, along with the ability to interact with colleagues outside the operating room. These results show that MR technology can be applied to customized and personalized surgical protocols, which is an essential guide for our experiments.

In summary, regarding the use of AI technologies in medicine, IoT platforms, digital twin technologies, and mixed reality technologies have become well established. In treatment, there are cases where one or more of the four technologies are sometimes used simultaneously to ensure accuracy [48][49]. This paper investigates the quantification and processing of data on lung cancer combined with pulmonary embolism in Yunnan and Chongqing provinces with the help of these four technologies to create a platform capable of experimenting with customized medical solutions.

III. New System Design

In this section, the diagnostic model of a digital twin-based lung cancer patient with PE, which is designed and implemented on intelligent IoMT through MR and a deep neural model, is demonstrated in Fig. 1. A new DLI-based rAC-GAN model is used to predict PE in lung cancer patients, and then an MR-based remote platform is deployed for diagnosis. Thereafter, 5G transmission based on the HUAWEI Cloud is employed for the transfer and computation of LC patients with a PE prediction.

A. Learning-based Intelligent Preoperative Diagnosis System for LC Patients with PE

The setup process of this preoperative diagnosis system is demonstrated in Fig. 2. The primary strategy of this system is threefold: 1) cleaning of clinical data collected manually, 2) novel upsampling and downsampling deep learning-based imputation to balance unbalanced data (here, a fill-in approach is used) and to eliminate the impact of sample imbalance on the predictive performance of retrospective cohorts of LC subjects and LC+PE subjects, and 3) a customized deep learning module for the classification task of LC+PE.

This article has been accepted for publication in a future issue of this journal, but has not been fully edited. Content may change prior to final publication. Citation information: DOI 10.1109/JIOT.2022.3176300, IEEE Internet of Things Journal

1) Preprocessing for Deep Learning-based Missing Data Imputation and Resampling

Recording incorrect clinical data tends to be inevitable because of some unexpected events, such as broken statistical systems or human-made mistakes. It will lead to the lack of sufficient samples for model training due to that the entire data is deleted only because the data of one patient is incomplete. In this work, a state-of-the-art deep learning-based imputation (DLI) method is used to fill in missing data. DLI can provide higher precision than conventional imputation methods because of its strong nonlinear approximation capabilities and can complete missing values at the character level [48]. It is mainly divided into three parts: 1) numerical encoding (if needed), 2) feature extraction, and 3) imputation model. In the numerical encoding part, the string data in column j are transformed into a representation $x^j \in \{1, 2, \dots, N_j, N_{j+1}\}$, where x^j is the index of the value in column j, N_j is the size of the histogram of x^j and N_{j+1} represents the missing data. The feature prediction part is essential since DLI can perform surprisingly well if the significant features can be extracted appropriately before the training and prediction of the model. A mapping $\emptyset_j(x^j) \in R^{D_j}$ for specific feature extraction is performed, where D_j represents the dimensionality associated with a latent variable of column$j$ and $\emptyset_j(\cdot)$ is defined as an embedding layer fed into a single fully connected layer [49]. Then, all mapping results $\emptyset_j(x^j)$ are concatenated into a feature vector:

$$\tilde{x} = [\emptyset_1(x^1), \emptyset_2(x^2), \dots, \emptyset_C(x^C)] \in D$$

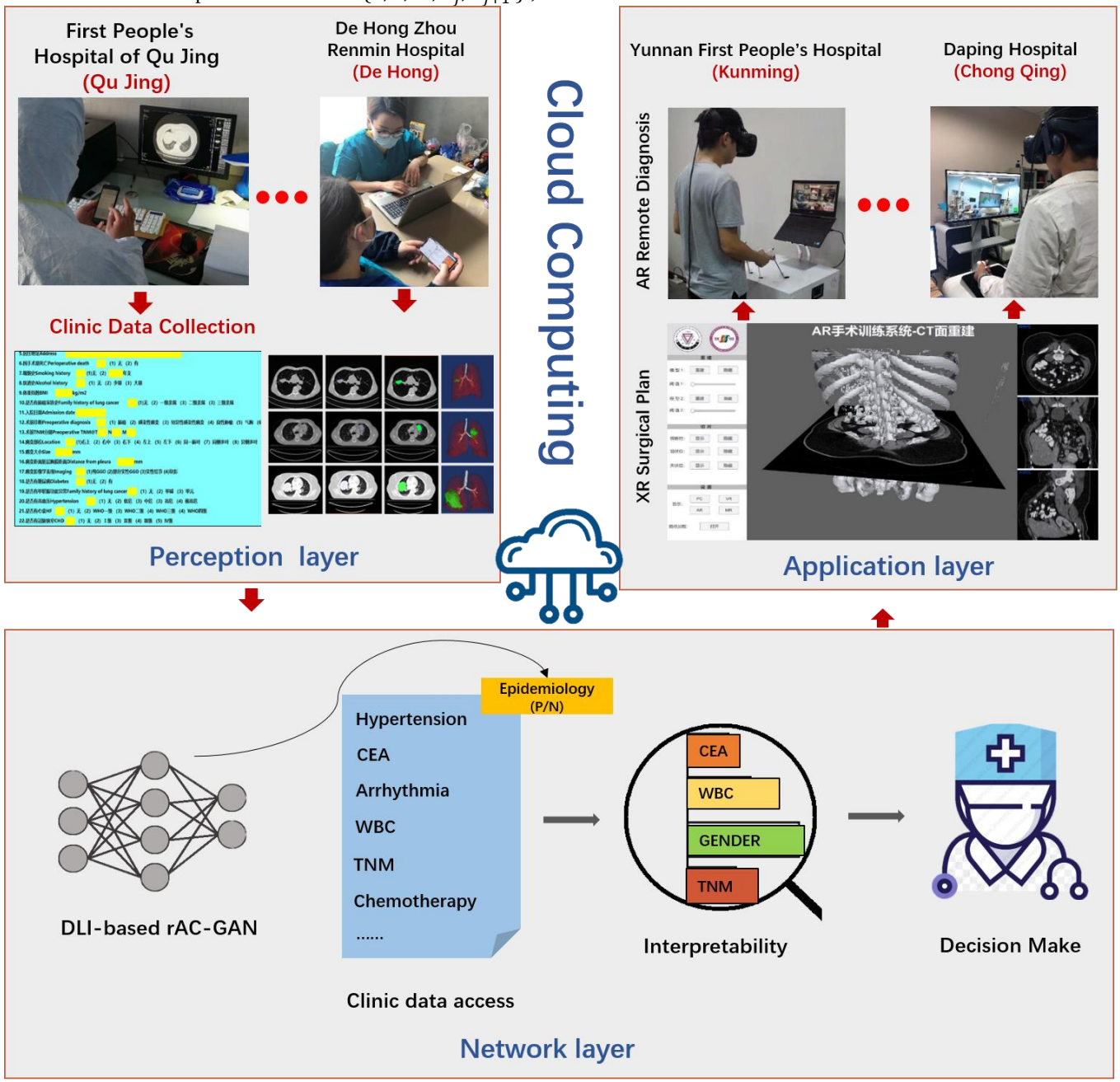

This article has been accepted for publication in a future issue of this journal, but has not been fully edited. Content may change prior to final publication. Citation information: DOI 10.1109/JIOT.2022.3176300, IEEE Internet of Things Journal

Fig. 1 Customized LC with PE Diagnostic Intelligent IoMT through MR and an artificially intelligent network, which has been applied to the prevention and treatment of LC with PE in Yunnan. The perception layer was used in areas with a high incidence of lung cancer, especially in Qu Jing and De Hong. Patient-specific data were gathered from the OPC of the perception layer using mobile phones, laptops, and tablets. After that, 5G transmission was used to transfer the surgical images and calculate the clinical data in real-time for lung cancer prediction using the 5G cloud (HUAWEI Cloud). Third, professional respiratory residents and thoracic surgeons from the application layer detail surgical treatment through the Intelligent IoMT application layer with high efficiency and safety.

where D is the result of summing all latent dimensions D_j. $y \in \{1, 2, \dots, D_i\}$ refers to the numerical representation of the values that are in the target column to be ready for imputation. Finally, the imputation model is established as follow:

$$p(y|\tilde{x}, \alpha) = softmax(W\tilde{x} + b)$$

As we know, the $softmax(.)$ can be described as:

$$softmax(q) = \frac{e^{q}}{\sum_m e^{q_m}}$$

Fusing the above two equations yields:

$$p(y|\tilde{x}, \alpha) = \frac{e^{(W\tilde{x}+b)}}{\sum_m e^{(W\tilde{x}+b)_m}}$$

where $\alpha = (W, z, b)$ is the learned parameters, which consist of all parameters about the learned column features $\emptyset_j$ and can be computed by learning the minimum of the cross-entropy loss between labels y and the distribution of prediction values:

$$\alpha = \arg\min_{\alpha} \sum_{1}^{n} -\log\left(p(y|\tilde{x}, \alpha)\right)^{T} onehot(y)$$

where $onehot(y)$ is used to maintain the continuity of label y. As it is fed into the network for training, $\arg min(.)$ indicates the minimum value index, which is used to output the index of the minimum value in a set of data.

DLI first removes some redundant data (undersampling) and then adds samples from the class to the lesser data (oversampling) in cases where the distribution of data samples is severely disproportionate; this widely used model is defined as resampling.

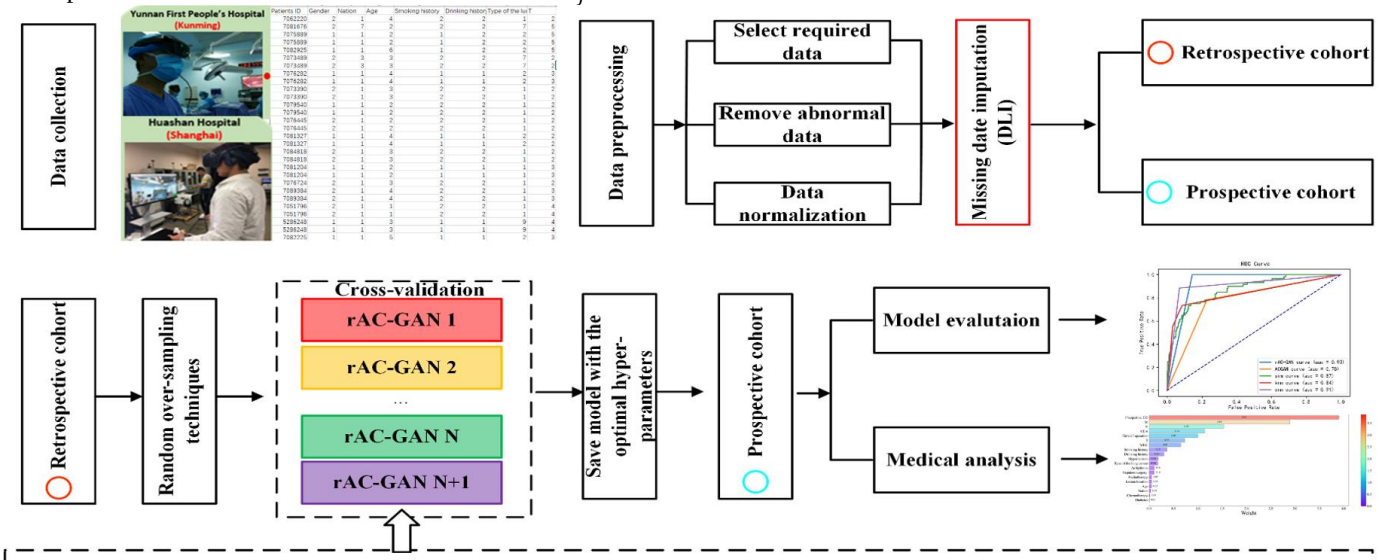

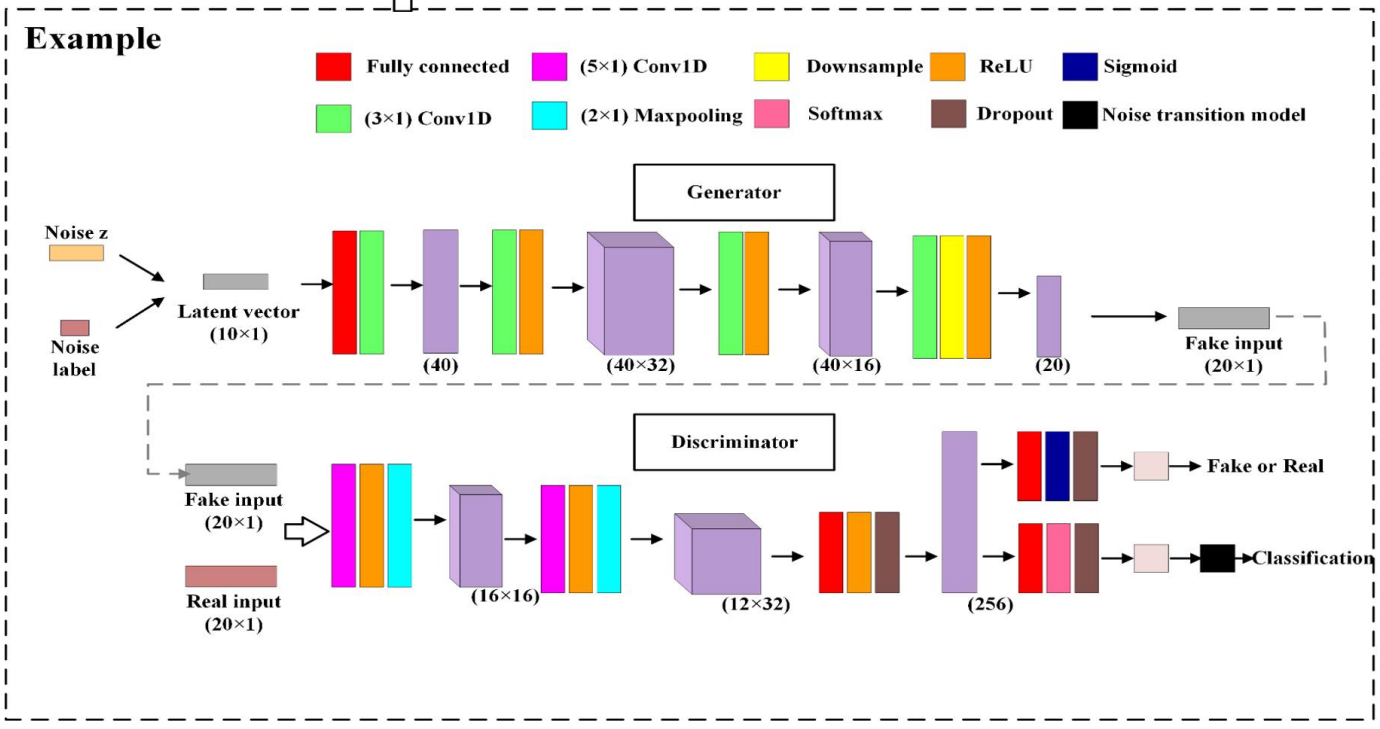

This article has been accepted for publication in a future issue of this journal, but has not been fully edited. Content may change prior to final publication. Citation information: DOI 10.1109/JIOT.2022.3176300, IEEE Internet of Things Journal

Fig. 2 Diagram of our real-time rAC-GAN-based preoperative diagnosis system for LC patients with PE.

2) Deep Neural Network Training Module

Deep learning techniques have been widely used in medicine, such as high-performance pathological diagnosis, to improve the workflow of health systems. In this paper, up-to-date deep learning, namely, a label-noise rAC-GAN, is employed in our system. A rAC-GAN is a modified network based on an AC-GAN that incorporates a noisy transition model into the discriminator to improve the robustness of the model. The additional ability of the rAC-GAN classifies the category of samples by expanding an auxiliary judgment layer in the discriminator [50]. Before the explanation of a rAC-GAN, some notations are defined. Throughout, we use $x \in \chi$ to denote the target data, $y \in \{1, 2, \dots, n\}$ to represent the real label in which $\chi \in \mathbb{R}^d$represents the space of the target data ($d$is the dimension) and n is the total number of classes. The superscript r is used to denote the real distribution and g denotes the generative distribution. $M = (M_{i,j}) \in [0,1]^{n\times n}(\sum_i M_{i,j} = 1)$ is defined as the label-noise transition matrix. A rAC-GAN can be optimized using two different loss functions: the adversarial part and the auxiliary part. In the adversarial part, the generator G and discriminator D start a zero-sum game. G tries to generate fake data that are indistinguishable by D, and D strives to find a boundary that can correctly distinguish between the real and generated data. The adversarial loss of the rAC-GAN is formulated as follows:

$$\mathcal{L}_{rAC-GAN} = \mathbb{E}_{x^r\sim p^r(x)}[logD(x^r)] + \mathbb{E}_{z\sim p(z),y^g\sim p(y)}[log\ (1 - D(G(z, y^g)))]$$

where x^r, z, y^g represent the distribution of the real data, the noise vector for $G(\cdot)$ and the generative distribution of a label, respectively; x and y are the actual data and its corresponding label; and $p(\cdot)$ is the probability density function. Where $\mathbb{E}$ denotes the mathematical expectation as follows: $\mathbb{E}(x) = \sum_{k=1}^{\infty} x_k * p_k$ where x_k denotes the value of x at index k and p_k denotes the probability of x occurring at index k. We can see by the formula that the value of $\mathcal{L}_{GAN}$ is related to the values of $\mathbb{E}_{x^r\sim p^r(x)}[logD(x^r)]$ and $\mathbb{E}_{z\sim p(z),y^g\sim p(y)}[log\ (1 - D(G(z, y^g)))]$. Since the data generated by G needs to be infinitely close to the true distribution of the data, the value of $\mathcal{L}_{GAN}$ needs to be the smallest.

The auxiliary part achieves the goal of generating data belonging to the target class, but a rAC-GAN has a large difference from an AC-GAN model. A rAC-GAN constructs a clean label generator by incorporating a noise transition model $p(\tilde{y}|y)$ into an auxiliary model when it is optimized by the classification loss on real data $\mathcal{L}_{rAC}^r$:

$$\mathcal{L}_{rAC}^r = \mathbb{E}_{(x^r,\tilde{y}^r)\sim p^r(x,\tilde{y})}[-log\tilde{C}(\tilde{y} = \tilde{y}^r|(x^r)]$$
$$= \mathbb{E}_{(x^r,\tilde{y}^r)\sim p^r(x,\tilde{y})}[-log\sum_{y^r} p(\tilde{y} = \tilde{y}^r|\hat{y} = \hat{y}^r)\hat{C}(\hat{y}^r|x^r)]$$

where $\tilde{C}$ is the classifier of a noisy label, $\hat{C}$ is the classifier of clean label, $\tilde{y}^r$ is the noise label with real distribution,$\hat{y}$ is the clean label. And we use $M_{y^r,\tilde{y}^r}$ to represent a probability where each clean label $\tilde{y}^r$ is polluted by a noise label $\tilde{y}^r$ [51]. Since the cross-entropy loss function is utilized in the rAC-GAN, which is a kind of proper composite loss [52], we can convert the above loss function into the original loss function under a clean distribution. The transition is formulated as follow:

$$\mathcal{L}_{rAC}^r = \mathbb{E}_{(x^r,\tilde{y}^r)\sim p^r(x,\tilde{y})}\left[-log\sum_{\hat{y}^r} M_{\hat{y}^r,\tilde{y}^r}C(\hat{y} = \hat{y}^r|x^r)\right]$$
$$= \mathbb{E}_{(x^r,\hat{y}^r)\sim p^r(x,\hat{y})}\left[-log\hat{C}(\hat{y} = \hat{y}^r|x^r)\right]$$

The main idea of this transition is that the process of minimizing $\mathcal{L}_{rAC}^r$ on samples with noisy labels can help us to obtain $\hat{C}$ that can classify x based on a clean label $\hat{y}$. Then, the part of the optimization of G on classification loss C can be formulated as:

$$\mathcal{L}_{rAC}^g = \mathbb{E}_{z\sim p(z),\hat{y}^g\sim p(\hat{y})}[-logC(\hat{y} = \hat{y}^g|G(z,\hat{y}^g))]$$

where y^g is the label with a generative distribution. Based on the above settings, the objective can be defined as follows:

$$\mathcal{L}_{D\&C} = -\mathcal{L}_{GAN} + \lambda_{AC}^r\mathcal{L}_{rAC}^r$$
$$\mathcal{L}_{D\&C} = \mathcal{L}_{GAN} + \lambda_{rAC}^g\mathcal{L}_{rAC}^g$$

where λ_{AC}^r and λ_{rAC}^g are the trade-off parameters. In a rAC-GAN, the clean classifier $\hat{C}$ is used to optimize G. Therefore, learning that $\hat{y}^g$ represents clean labels is encouraged.

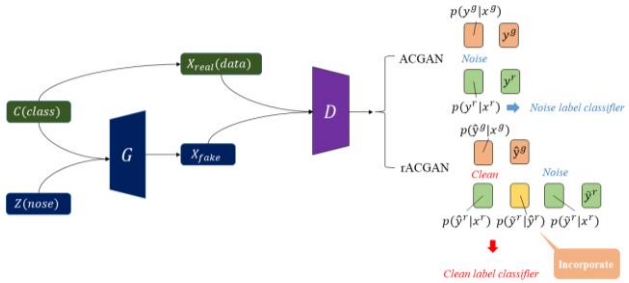

Fig. 3 The AC-GAN model and the rAC-GAN model are similar before the discriminator. The information shown on the left side of Fig. 3 is the process of generating data using the whole generator for both models. The data X_{fake} generated by the generator and the real data $X_{real}(data)$ are fed to the discriminator. On the right side of Fig. 3, the difference between the AC-GAN model and the rAC-GAN model is shown, where the outputs (labeling and classification) of both models are the same. The difference is shown in the figure where the rAC-GAN model has a cleanup process for the labels before the label distribution output.

The differences between the AC-GAN and rAC-GAN models in terms of discriminators are shown in Fig. 3. In the generator part for the input data, both models have the same structure. In the discriminator part, the rAC-GAN adds a noise transition module. The function of this module is to process the output distribution, clean up the redundant predictive distribution in it, and extract a predictive distribution that is more consistent with the true distribution. In principle, the processing of the rAC-GAN at the prediction distribution can be illustrated by transforming $P(\hat{y}^r|x^r)$ to $P(\tilde{y}^r|\hat{y}^r)$ to $P(\tilde{y}^r|x^r)$ into $P(\tilde{y}^r)$. $P(.)$ represents the conditional probability distribution in statistics. In the conditional probability distribution, $P(A|B)$ represents the probability of occurrence of event A under the condition that event B has occurred. In this study, we use $P(\tilde{y}^r|\hat{y}^r)$ to clean up the noise in the distribution $\hat{y}^r$ that has been obtained, resulting in a more accurate classification result $\tilde{y}^r$. The probability of $P(\tilde{y}^r)$ is subsequently obtained to clean up the predictive distribution. The distribution of results after the discriminator predicts the data is represented by x^r.

This article has been accepted for publication in a future issue of this journal, but has not been fully edited. Content may change prior to final publication. Citation information: DOI 10.1109/JIOT.2022.3176300, IEEE Internet of Things Journal

TABLE I HOW THE DLI-PROCESSED DATA IS PROCESSED AFTER IT IS FED INTO THE RAC-GAN MODEL

	Genetic Code Evolution
1	**for** *train.shape[0]/batchsize* **do**
2	#generator
3	The generator generates the text data we need using randomly generated *noise* z that matches a Gaussian distribution.
4	#discriminator
5	The generated dataX_f and the real data X_t are input into the discriminator at the same time, and the *validity* and *label* of the results are obtained (*validity* is used to determine *fake* and *real*, and *label* is used to assist in classification).
6	**if***(the rate of real)>(the rate of fake)***do**
7	discriminator output label **then**
8	a =*np.argmax(label)*
9	**delete** the number **if**a == 0
10	**return** a

The process of the rAC-GAN for lung cancer combined with pulmonary embolism data is described in Table I. First, the generator processes the input noise z and classification labels and outputs the false data x. We input the false data x_{fake} and the real data $x_{real}(data)$ together into the discriminator and finally output two sets of data: the validity and label. We need the label data for the final classification task. The output of the classification result by the discriminator is based on the classification distribution after noise processing. Therefore, compared with the results of AC-GAN, the accuracy has been greatly improved.

3) Contrast of Explanation Methods for the Prediction System

A novel explanation algorithm, named the contrastive explanations method (CEM), was developed by IBM [53]. The CEM is regarded as an optimization problem by adding perturbation value δ to look for the positive/negative correlation between input features and the incidence of LC patients with PE in the deep learning model. An analysis of pertinent negatives (PN), X refers to the feasible data; we define $(x_0, y_0), x_0 \in X$ as an example in which y_0 represents the class label predicted by the deep learning model; $x \in X$ is defined as modified feasible data, which is perturbation variable δ plus x_0: $x = x_0 + \delta$ and $y_\delta$is the prediction results of the model. For any input x, the CEM is devoted to discovering an interpretable perturbation and thus studying the prediction difference between $argmax_i[Pred(x_0)]_i$ and $argmax_i[Pred(x_0 + \delta)]_i$, where $Pred(\cdot)$ is the model prediction that is made up of probabilities for all classes. The implementations of the CEM are defined as follows:

$$\mathcal{L} = \min_{\delta \in X/x_0} c \cdot f_k^{neg}(x_0,\delta) + \beta\|\delta\|_1 + \|\delta\|_2^2 + \gamma\|x\text{-}AE(x)\|_2^2$$

where $\mathcal{L}$ is an objective function designed to find proper x which leads to patients to be predicted as a different class than $y_0 = argmax_i[Pred(x_0)]_i$; $[Pred(x_0, \delta)]_i$ refers to the probabilities of the i-th class of x; k refers to confidence parameter controlling the separation between $[Pred(x)]_{y_0}$and $\max_{i \neq t_0}[Pred(x)]_i$; $\beta\|\delta\|_1$; and $\|\delta\|_2^2$ is designed as an elastic regularizer, a parameter used in high-dimensional learning problems for feature selection.

B. Digital Twin-based LC with PE Remote Surgical Platform.

The overall network structure of the IoMT is shown in Fig. 1 and includes a perception layer, network layer, and application layer. The whole structure of the network is subsequently explained layer-by-layer. The role of the perception layer is to collect customers' medical data while preprocessing (deleting, filling, etc.). It is responsible for collecting customers' comments after use and feeding them back to the network layer to improve the prediction accuracy of the network layer. In the structure of this paper, the network layer adopts a stepped structure, which includes the following. 1) A DLI structure with strong anti-interference capability for predicting the collected customer medical data. 2) A CLOUD, which is used to connect the DLI of the backend and application layer. With the support of 5G technology, the network latency of both can be controlled below milliseconds. 3) Digital twin technology is incorporated to create a personalized digital twin of the customer. The application layer mainly serves users to experiment with customized medical solutions and feeds back their opinions to the perception layer to form a specific medical service system. The cyclic structure of the IoMT in this paper is as follows. The perception layer coordinates data to update and improve the whole network layer, and then the updated network layer is applied to the application layer to achieve the purpose of the IoMT, obtain technology updates in real-time, and improve the real-time digital twin technology. In the following, the construction of the digital twin and the IoMT network will be presented.

1) Patient-specific Digital Twin-based CT Rendering

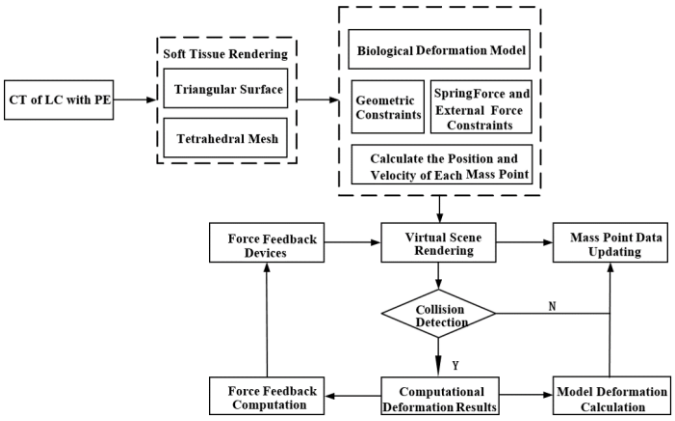

Fig. 4 Flow chart of the digital twin-based surgery simulation system showing the integration of the digital twin-based remote surgery architecture with smart IoMT device implementation. Complete lung cancer combined with pulmonary embolism data is the input for soft tissue presentation, and then a physical deformation model is built. There are three key points in building the biomorphic model: geometric constraints, spring force, and external force constraints, and calculating the position and velocity of each mass. The flowchart in the lower half shows how to better obtain the three key points in the construction of the biomorphic model.

Our data are provided by the First People's Hospital of Yunnan Province, the Third Military Medical Ta Ping Hospital, and the First People's Hospital of Qujing. Based on the clinical test characteristics provided by the physicians, we extracted data on age, sex, risk factors, d-dimer levels, electrocardiogram (ECG), TNM staging, white blood cells, pathological staging, pathological sites, and chest imaging

This article has been accepted for publication in a future issue of this journal, but has not been fully edited. Content may change prior to final publication. Citation information: DOI 10.1109/JIOT.2022.3176300, IEEE Internet of Things Journal

manifestations from the patients' electronic medical records (EMRs). These data were recorded between 1992 and 2019.

Since the patient-specific data are collected manually, which may cause various mistakes in the data computation, we also invited four experienced doctors to check the data reliability. The CT images for the hospital's visual rendering in Fig. 5 demonstrate the digital twin-based rendering of a human lung model. The marching cube algorithm is utilized for the 3D mesh reconstructed model, which is implemented in OpenGL [54]. VTK, CTK, ITK, and IGSTK packages are also integrated into the simulation for medical image processing for visual rendering.

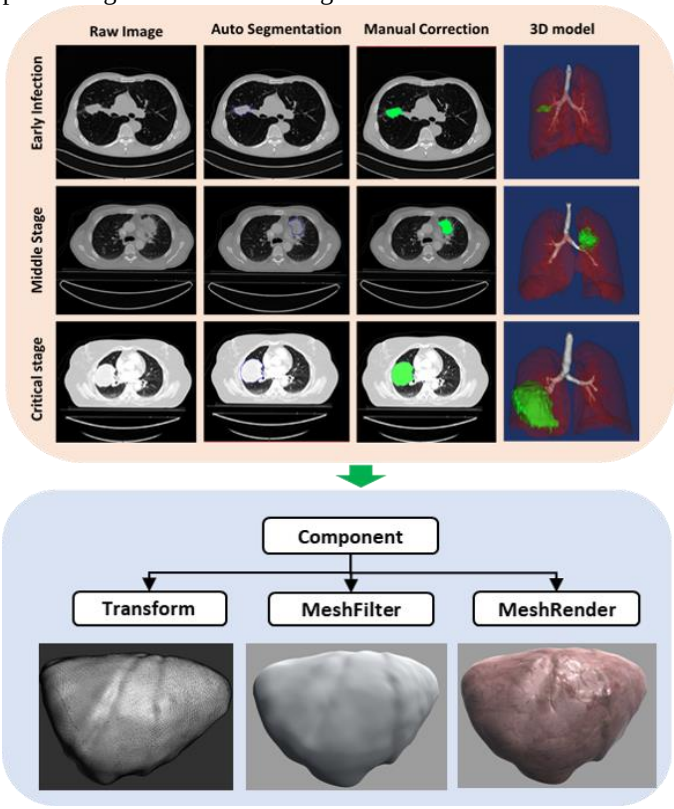

Fig. 5 Patient-specific digital twin-based CT rendering from the perception layer. The second part shows the MR visual-haptic reconstruction with medical data.

2) IoMT-based MR Simulator Hardware Design

The IoMT-based MR simulator is designed and implemented in the surgeons' application layer to perform remote diagnoses. To achieve tactile replication for the digital twin system after rendering the visual framework, we also need to integrate a haptic force feedback framework. Due to the great difference in refresh rate between the visual (~60 Hz) and haptic rendering (~1000 Hz), an asynchronous transmission mechanism is used in the system design [55][56]. An Openhaptic plugin is developed for graphic and haptic integration and real-time surgical force rendering. The real surgical instruments for the operation are integrated into the hardware system, which is shown in Fig. 6. The surgeon can use a Maryland dissector, which is the same as in the perception layer, and feel the same force rendering as the real lung cancer patient. Fig. 6 shows the IoMT-based MR simulator we developed. The 3D model of the connector is shown in Fig. 6 (G\F). When the operator closes the surgical instrument, the green button will be triggered, and the virtual instrument will close as if grabbing a virtual object. When the operator opens the surgical instrument, the red button will be activated, and the virtual instrument will be opened as if releasing a virtual object.

Fig. 6 IoMT-based MR simulator hardware design: A) Touch screen with an 8K resolution. B) Logitech camera (Logitech, Switzerland) for identifying markers for AR development. C) Marker. D) HTCVIVE virtual reality headset (HTC Corporation, Taiwan, China). E) Maryland dissector surgical instruments. F) Geomagic Touch (Geomagic, USA) force feedback devices with six degrees of freedom (6-DoF). G) Linker between force feedback and surgical instrument. H) Desktop computer with an NVIDIA GTX 2060 GPU, Intel i7CPU, and 16 GB RAM.

IV. Results

A. Model Performance Evaluation

After filling the lung cancer combined with pulmonary embolism data using the DLI, they were imported into representative machine learning and deep learning networks (KNN, DNN, SVM), and the results were obtained as shown in Fig. 7 and Table II. The results in Fig. 7 and Table II are analyzed in turn.

The receiver operating characteristic - area under the curve (ROC-AUC) graph obtained from the data predicted using different models is shown in Fig. 7. The ROC curve is also called the receptivity curve, where the points on the curve reflect the same receptivity, and the AUC is used to measure the "binary classification problem" and its learning algorithm performance. Comparing the results in Fig. 7, it can be seen that the rAC-GAN has the best performance among all networks with a score of 0.93, and the value of the ROC curve of the network surpasses the AC-GAN model by 0.15 and the DNN by at least 0.02. In summary, we can conclude that rAC-GAN has a strong superiority in the processing of the filled

This article has been accepted for publication in a future issue of this journal, but has not been fully edited. Content may change prior to final publication. Citation information: DOI 10.1109/JIOT.2022.3176300, IEEE Internet of Things Journal

lung cancer combined with pulmonary embolism data.

The data in Table II show the differences of each network in terms of accuracy, precision, recall, and F1 parameters, where the network we used (rAC-GAN) scored the highest in accuracy, indicating that this network is a very effective classifier. Accuracy and recall are usually in a reciprocal relationship, and to illustrate the effectiveness of the experimental method, we generally use the F-measure. F1 is used in this paper to obtain a weighted summed average of accuracy and recall. The rAC-GAN's performance in the last three datasets shown in Table II is not the best, but it is average.

By analyzing the data in Figure 7 and Table II, it is concluded that rAC-GAN performs very well in classifying lung cancer combined with pulmonary embolism data, compared with conventional machine learning and deep learning networks. The results further demonstrate that it is reliable to build a surgical platform based on the results of the rAC-GAN network after classification.

TABLE II THE DIFFERENCES IN ACCURACY, PRECISION, RECALL, AND F1-SCORE VALUES FOR DIFFERENT MODELS. THE DATA FROM THE TABLE SHOW THAT the rAC-GAN HAS THE BEST DATA PERFORMANCE AMONG ALL MODELS

Model	Accuracy	Precision	Recall	F_1-score
KNN	0.65	0.71	0.62	0.66
SVM	0.69	0.71	0.65	0.68
DNN	0.84	0.82	0.79	0.80
AC-GAN	0.82	0.39	0.93	0.55
rAC-GAN we used	0.92	0.57	0.73	0.64

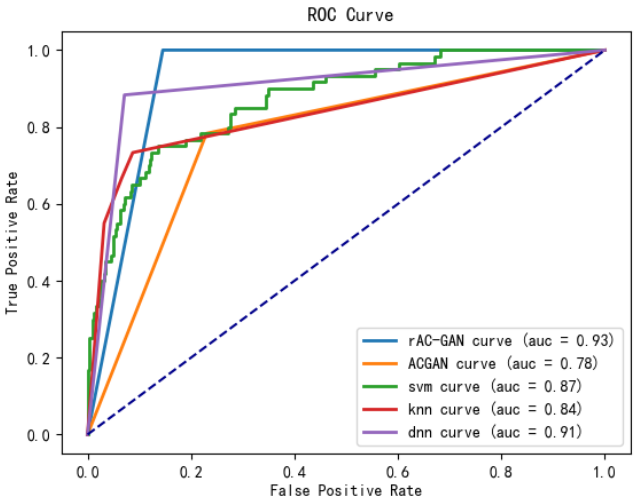

Fig. 7 The values of ROC curves and AUCs predicted using different models for the completed lung cancer combined with pulmonary embolism data. In the results, both the ROC curve and the value of the AUC were the best using the rAC-GAN model.

To test the effectiveness of the DLI for missing clinical data, we executed a performance comparison between DLI-based prediction and KNN-based prediction. The details for the comparison results are displayed in Table III. A novel error measurement, forecasting skill (FS), is used to calculate the improvement percentage by comparing DLI-based prediction with KNN-based prediction. The formula for FS is shown below:

$$FS_{DLI\ imputation} = \frac{Model_{DLI\ imputation} - Model_{KNN\ imputation}}{Model_{KNN\ imputation}}$$

From the above equation, it is shown that DLI-based prediction is better than KNN-based prediction when the obtained result is positive. Table III shows that DLI-based imputation can bring a prominent promotion apart for SVM and XGB. The promotion for LR was the largest, which rose by approximately 20% for all evaluation metrics. Moreover, it helps our rAC-GAN obtain nearly 8% promotion on the current prediction task. All the results demonstrate that DLI imputation has superior performance to the famous KNN-based imputation method.

TABLE III. VALUES OF DIFFERENT INDICATORS OUTPUTTED BY THE TARGET MODEL.

DLI imputation vs. KNN imputation	$FS_{accuracy}$	$FS_{precision}$	FS_{recall}	$FS_{F1\text{-}score}$
KNN	0.10	0.03	0.09	0.06
LR	0.24	0.27	0.20	0.26
SVM	-0.04	0.08	-0.10	0.00
RF	0.02	0.04	0.05	0.04
XGB	0.02	0.05	-0.05	-0.05
DNN	0.06	0.07	0.08	0.04
CNN	0.11	0.14	0.04	0.06
rAC-GAN we used	0.06	0.08	0.10	0.08

B. Robust Performance

In this section, we experiment to test the robustness of our model. The concrete procedures are as follows: (1) 60% of our dataset was selected randomly as a retrospective cohort, and the remaining were prospective cohorts. (2) The retrospective cohort was used to train the eight prediction models. (3) The prospective cohort was used to assess the performance of these models using F_1-score metrics. (4) We repeated steps (1)-(3) 30 times. The length of the vertical icon in Figure 8 indicates the change in the floating f1-score values for each model over 30 experiments. From the figure, we find that the floating of the results of the rAC-GAN network over 30 experiments ranges from 0.75 to 0.85. The rAC-GAN has very high robustness compared to all the models used for the experiments.

This article has been accepted for publication in a future issue of this journal, but has not been fully edited. Content may change prior to final publication. Citation information: DOI 10.1109/JIOT.2022.3176300, IEEE Internet of Things Journal

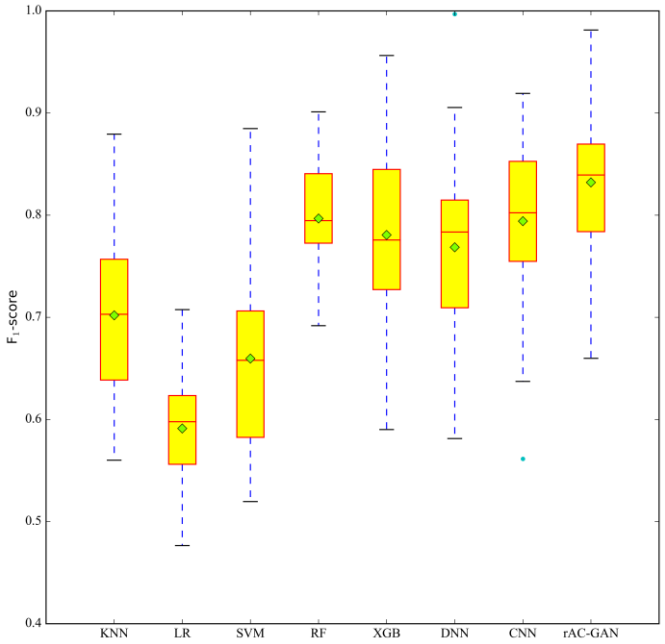

Fig. 8 Thirty experimental results of the robustness test for different algorithms.

V. Discussion

A deep learning network-based framework has been proposed to design a digital twin-enabled intelligent IoMT system for telemedical simulation. After training, LC with PE can be precisely predicted with or without assistance using the IoMT and the medical analysis results for patient data, which can be provided before the beginning of the operation. Based on the prediction results and our medical analysis system, experts can provide remote visual and numerical feedback via our IoMT application layer.

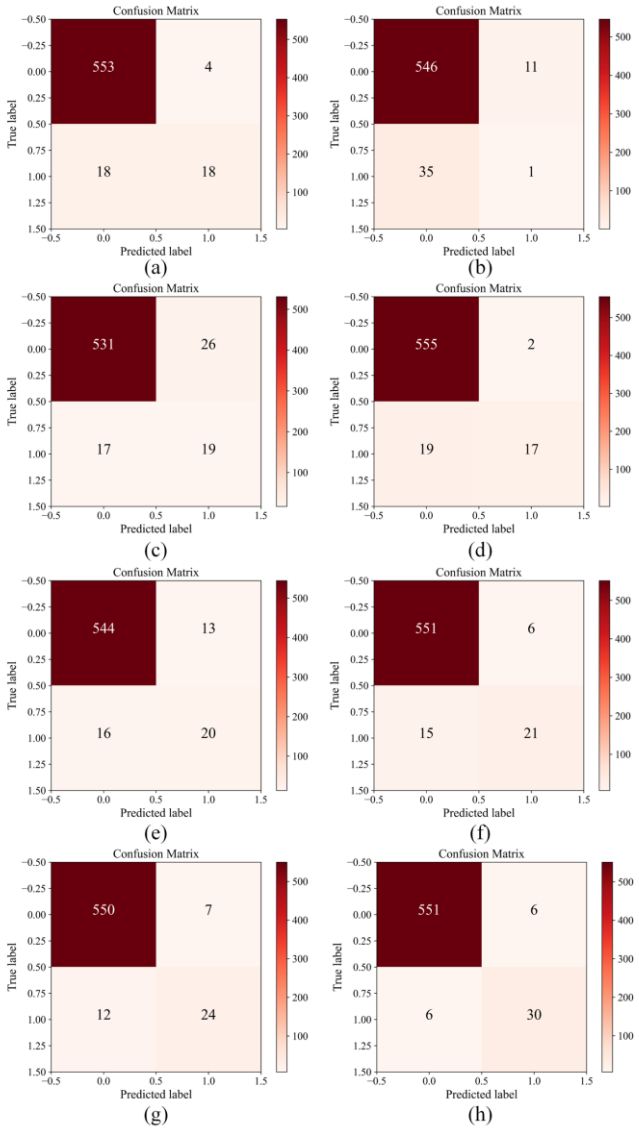

Fig. 9 Confusion matrix for the different algorithms: (a) KNN, (b) LR, (c) SVM, (d) RF, (e) XGB, (f) DNN, (g) CNN, (h) rAC-GAN.

A. Performance of the rAC-GAN-based LC with PE System

Based on Table II, Table III, Fig. 8, and Fig. 9, it can be concluded that the DLI-rAC-GAN model has excellent performance and strong robustness. Next, we analyze each result layer-by-layer.

Table II shows that the accuracy of the rAC-GAN is improved by 8% compared to the traditional DNN deep learning model. In principle, compared with the DNN, which only has a single convolutional layer to extract features, the rAC-GAN uses adversarial training based on Nash equilibrium, and the output labels used for auxiliary classification go through a noise transition model to clean up the noise. Therefore, it has higher evaluation metrics than the DNN. Compared with the most popular SVM in medicine, the accuracy of the rAC-GAN is improved by 23%. Compared to the SVM, the rAC-GAN belongs to a deep learning network, which has two significant advantages: 1) more accurate extraction of data features and 2) more training layers for deep iterations and more adequate training of data. These results show that the rAC-GAN can achieve high prediction accuracy.

This article has been accepted for publication in a future issue of this journal, but has not been fully edited. Content may change prior to final publication. Citation information: DOI 10.1109/JIOT.2022.3176300, IEEE Internet of Things Journal

The rAC-GAN has an AUC of 93%, which is the highest value among all models.

Comparing the DLI attribution-based method with the KNN attribution method, we obtained the data shown in Table III by subtracting the obtained values of the two. It is easy to see that almost all models using the DLI attribution method have improved performance (from 2% to 27% compared to the KNN attribution method), except for the accuracy and recall of the SVM and the recall F1 score of the XGB. Therefore, we can conclude that the DLI-based attribution method provides a more appropriate complimentary strategy than the KNN-based attribution method. As mentioned above, since DLI fills the missing data with a nonlinear approximation, the filled data are closer to the original data and can give us better results. The results in Table III similarly demonstrate the strong robustness of the DLI-rAC-GAN in predicting the performance under the current task.

To test whether the rAC-GAN is strongly robust to interference, we conducted 30 randomized experiments to obtain the results shown in Fig. 8, sharing the most obvious median and mean in terms of F1 scores. Therefore, we can conclude that the rAC-GAN is strongly robust to interference. This conclusion can likewise be obtained from the confusion matrix shown in Fig. 9, from which we can see that the rAC-GAN has almost no misclassification, with only 12 errors out of a total of 593 patients. We can also see from Figure 9 that KNN has 22 data classification errors; LR has 46 classification errors; SVM has 43 classification errors; RF has 21 classification errors; XGB has 29 classification errors; DNN has 21 classification errors, and CNN has 19 classification errors. From the above classification results, we can conclude that the rAC-GAN network has high classification accuracy.

B. *Model Interpretability and Feature Analysis*

Unlike other tasks, the results of misprediction in medical diagnoses may be fatal. In addition to the desire for higher accuracy, the requirements of rationality, which are the top priority for physicians to judge whether a prediction model can be relied on, are vital for practice. Therefore, it is important to visualize how the black box understands and gives its opinion on these clinical features. High-trust judgment of clinical features gives physicians insight and further helps them provide treatment strategies for their patients more effectively and accurately. The results of the system predictions were compared and interpreted using the CEM method, and the conclusions drawn are shown in Fig. 10. The results are highly similar to meta-analysis, a highly recognized method to analyze the correlation between features and disease in medicine in LC with PE. It is fully proven that our proposed system not only has accuracy but also has responsibility. It can be demonstrated that the use of AI for clinical medicine as an aid to diagnosis and treatment makes it feasible. There is experimental evidence that the extraction of features in a dataset using an AI algorithm is essentially the same as those extracted by an experienced clinician. It even exceeds the average performance of radiologists in some metrics [57]. The results showed that the most relevant features in machine learning are preoperative DD, hypertension, time to surgery, M, CEA, surgery, and WBC. Sex, T stage, diabetes, arrhythmia, age, and country were least relevant.

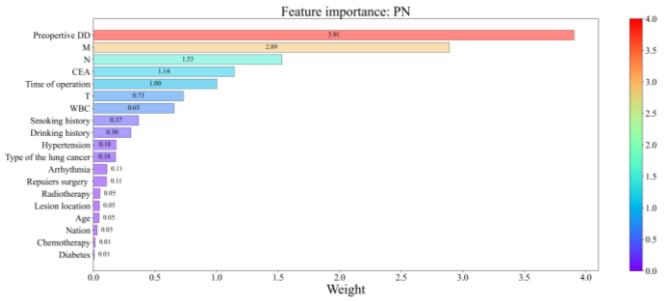

Fig. 10 The clinical data analysis results of patients using CEM on the prospective cohort.

C. *Verification from the Statistical Results of Epidemiology*

The Statistical Product and Service Solution (SPSS) 22.0 statistical was employed for the deep neural network evaluation, and the results are shown in Table IV, along with stratified clinical characteristics of patients with lung cancer and lung cancer combined with pulmonary embolism. Data on 1372 cases of lung cancer and 90 cases of lung cancer combined with pulmonary embolism were included, for a total of 1462 patients (mean age 40-70 years). Combined with the experimental data, 35.7% of the patients with lung cancer were women with a mean age of 55 years; 34.7% of the patients with lung cancer combined with pulmonary embolism were women with a mean age of approximately 57 years. After p-value analysis, we found no apparent discrepancy in demographics, lung cancer risk factors, characteristics, or treatment of complications. Fig. 10 shows the features learned in our DLI-rAC-GAN model, and the top ten factors in order of prevalence are the preoperative DD, M, N, time of operation, CEA, WBC, smoking history, drinking history, and hypertension. The agreement between the selection of clinical features and the deep learning-based algorithm was 90%. This proves that our DLI-rAC-GAN network is feasible for building digital twin-assisted diagnostic treatment.

TABLE IV. EPIDEMIC AND CLINICAL CHARACTERISTICS OF LUNG CANCER AND LUNG CANCER PLUS PE FACTORS

Variable	Patients with lung cancer (n=1372)	Patients with lung cancer plus PE (n=90)	p-value
Nation minority	Han 1276(93)	85(94.4)	0.98
	Others 96(7)	5(5.6)	
Age (mean± SD)	57±13.37	55±13.37	0.03
T, n (%)	T0~2 591(43)	20(22.2)	**<0.001***
	T3~4 678(49.4)	37(41.1)	
	T4+ 85(6.1)	33(36.6)	
Females, n (%)	491(35.7)	33(36.6)	0.27
Smoking history, n (%)	625(45.5)	20(22.2)	0.000*
Drinking history, n (%)	409(29.8)	26(28.9)	0.55
N, n (%)	N0 792(57.7)	15(16.6)	**<0.001***
	N1~2	38(42.2)	

	522(38)		
	N3+ 39(2.8)	37(41.1)	
	M0 1269(92.4)	30(33.3)	
M, n (%)	M1 60(4.3)	29(32.2)	**<0.001***
	M2~6 24(1.7)	31(34.4)	
Preoperative DD(mean± SD)	1.97	19.94	**0.023***
Operative time (mean± SD)	2.54	4.96	**<0.001***
Lesion location			**0.003***
Radiotherapy, n (%)	41(2.98)	11(12.2)	**0.042***
CEA(mean± SD)	40.45	267.01	0.307
Surgery, n (%)	633(46.1)	13(18.8)	**<0.001***
Hypertension, n (%)	600	50	0.15
Arrhythmia, n (%)	220(16)	29(32.2)	0.32
Diabetes	94(6.8)	26(28.8)	0.012
Chemotherapy, n (%)	613(44.6)	31(34.4)	0.12
WBC(mean± SD)	12.37	11.32[9.82-12.81]	0.952

VI. Conclusion

In this study, we found that the clinical approach to impute DIL for missing data outperformed the traditional KNN imputation method. At the same time, it was also found that the IoMT digital twin customized surgical operation platform built with deep learning had higher accuracy. We performed a MATA analysis of the data and concluded that the features we used in our experiments were the same as the clinical features. However, in the research, we found that the IoMT surgical operation platform built with cloud technology had high requirements on the network transmission rate in real-time. When processing medical clinical data of various structures, the requirements for equipment configuration were high. Based on the above observations, we have the following prospects in the future: (1) The IoT technology based on the same local area network might be used to enhance the IoMT surgical platform based on cloud technology, reducing the requirements for network transmission rate; (2) Improve the utilization of code for reducing the demand for high-configuration equipment in the experimental part; (3) Strengthen the basis of the original deep learning network to further improve the accuracy and reliability of clinical diagnosis.

References

[1] Fuller A, Fan Z, Day C, et al. Digital twin: Enabling technologies, challenges and open research[J]. IEEE access, 2020, 8: 108952-108971.

[2] Suresh V , Ramson J , Jegan R . Internet of Medical Things (IoMT) - An overview[C]// 2020 5th International Conference on Devices, Circuits and Systems (ICDCS). 2020.

[3] Aslam A, Curry E. A survey on object detection for the internet of multimedia things (IoMT) using deep learning and event-based middleware: approaches, challenges, and future directions[J]. Image and Vision Computing, 2021, 106: 104095.

[4] Yang H H, Chen H. Research Progress of Lung Cancer Combined With Pulmonary Embolism[J]. Chinese journal of tuberculosis and respiratory diseases, 2020, 43(7): 577-581.

[5] Abdel-Basset, Mohamed, Chang, V. "HSMA_WOA: A hybrid novel Slime mould algorithm with whale optimization algorithm for tackling the image segmentation problem of chest X-ray images." Applied Soft Computing (2020): 106642.

[6] Chang, V. Computational Intelligence for Medical Imaging Simulations. J Med Syst 42, 10 (2018).

[7] Chang, V. Data analytics and visualization for inspecting cancers and genes. Multimed Tools Appl 77, 17693–17707 (2018).

[8] Y. Tai, K. Qian, X. Huang, J. Zhang, M. A. Jan and Z. Yu, "Intelligent Intraoperative Haptic-AR navigation for COVID-19 Lung Biopsy using Deep Hybrid Model," in IEEE Transactions on Industrial Informatics, doi: 10.1109/TII.2021.3052788.

[9] L. Liu, O. De Vel, Q.-L. Han, J. Zhang, and Y. Xiang, "De- tecting and preventing cyber insider threats: A survey," IEEE Communications Surveys & Tutorials, vol. 20, no. 2, pp. 1397–1417, 2018.

[10] S. Liu, J. Zhang, Y. Xiang, W. Zhou, and D. Xiang, "A study of data pre-processing techniques for imbalanced biomed- ical data classification." arXiv: Quantitative Methods, 2019.

[11] Tai Y, Gao B, Li Q, et al. Trustworthy and intelligent covid-19 diagnostic iomt through xr and deep-learning-based clinic data access[J]. IEEE Internet of Things Journal, 2021, 8(21): 15965-15976.

[12] Raj R J S, Shobana S J, Pustokhina I V, et al. Optimal feature selection-based medical image classification using deep learning model in internet of medical things[J]. IEEE Access, 2020, 8: 58006-58017.

[13] Minerva R , Lee G M , Crespi N . Digital Twin in the IoT Context: A Survey on Technical Features, Scenarios, and Architectural Models[J]. Proceedings of the IEEE, 2020, PP(99):1-40.

[14] Mathupriya S , Banu S S , Sridhar S , et al. Digital twin technology on IoT, industries & other smart environments: A survey[J]. Materials Today: Proceedings, 2020.

[15] Corral-Acero J , Margara F , Marciniak M , et al. The 'Digital Twin' to enable the vision of precision cardiology[J]. European Heart Journal, 2020.

[16] Zhang, L., Zhou, L., Ren, L., Laili, Y., 2019. Modeling and simulation in intelligent manufacturing. Comp. Indus. 112, 103123.

[17] Tao, F., Qi, Q., Wang, L., Nee, A.Y.C., 2019. Digital twins and cyber-physical systems toward smart manufacturing and Industry 4.0: correlation and comparison. Engineering 5 (4), 653661.

[18] Patrone C , Lattuada M , Galli G , et al. The Role of Internet of Things and Digital Twin in Healthcare Digitalization Process[M]. 2020.

[19] L. Zhao et al., “Indoor device-free passive localization with DCNN for location-based services,” The Journal Supercomputing, vol. 76, no. 11, pp. 8432–8449, 2020.

[20] Zhou F., Yang S., Fujita H., et al. Deep learning fault diagnosis method based on global optimization GAN for unbalanced data[J]. Knowledge-Based Systems, 2020, 187(Jan.):104837.1-104837.19.

[21] Anusha K. S., Ramanathan R., Jayakumar M. Impact of K-NN imputation Technique on Performance of Deep Learning based DFL Algorithm[C] 2021 Sixth International Conference on Wireless Communications, Signal Processing and Networking (WiSPNET). 2021.

[22] Bharathi M., Amsaveni A. Machine Learning with IoMT: Opportunities and Research Challenges[M]. 2021.

[23] Zhang L., Lin G., Gao B., et al. Neural Model Stealing Attack to Smart Mobile Device on Intelligent Medical Platform[J]. Wireless Communications and Mobile Computing, 2020, 2020(3):1-10.

[24] Akilandeswari J, Jothi G, Naveenkumar A, et al. Detecting Pulmonary Embolism using Deep Neural Networks[J]. International Journal of Performability Engineering, 2021, 17(3).

[25] Y. Li, Y. Shang, W. Wang, S. Ning, and H. Chen, "Lung cancer and pulmonary embolism: What is the relationship? A review," J. Cancer, vol. 9, no. 17, pp. 3046–3057, 2018, doi: 10.7150/jca.26008.

[26] Wang P, Zhao H, Zhao Q, et al. Risk factors and clinical significance of D-dimer in the development of postoperative venous thrombosis in patients with lung tumor[J]. Cancer Management and Research, 2020, 12: 5169.

[27] Li X, Wang X, Yang X, et al. Preliminary study on artificial intelligence diagnosis of pulmonary embolism based on computer in-depth study[J]. Annals of Translational Medicine, 2021, 9(10).

[28] I. Banerjee et al., "Development and Performance of the Pulmonary Embolism Result Forecast Model (PERFORM) for Computed Tomography Clinical Decision Support," JAMA Netw. Open, vol. 2, no. 8, pp. 1–14, 2019, doi: 10.1001/jamanetworkopen.2019.8719.

[29] F. Biessmann et al., "Machine Learning and Prediction of All-Cause Mortality in COPD," Chest, vol. 21, no. 3, pp. 952–964, 2018, doi: 10.7150/jca.26008.

[30] X. Wang et al., "Prediction of the 1-year risk of incident lung cancer: Prospective study using electronic health records from the state of Maine," J. Med. Internet Res., vol. 21, no. 5, 2019, doi: 10.2196/13260.

[31] P. Petousis, A. Winter, W. Speier, D. R. Aberle, W. Hsu, and A. A. T. Bui, "Using Sequential Decision Making to Improve Lung Cancer Screening Performance," IEEE Access, vol. PP, no. August, p. 1, 2019, doi: 10.1109/ACCESS.2019.2935763.

[32] Chen Z, Chen K, Lou Y, et al. Machine learning applied to near-infrared spectra for clinical pleural effusion classification[J]. Scientific reports, 2021, 11(1): 1-8.

[33] Liu W, Liu M, Guo X, et al. Evaluation of acute pulmonary embolism and clot burden on CTPA with deep learning[J]. European radiology, 2020, 30(6): 3567-3575.

[34] Abawajy J H, Hassan M M. Federated internet of things and cloud computing pervasive patient health monitoring system[J]. IEEE Communications Magazine, 2017, 55(1): 48-53.

[35] Durga S, Nag R, Daniel E. Survey on machine learning and deep learning algorithms used in internet of things (IoT) healthcare[C]//2019 3rd International Conference on Computing Methodologies and Communication (ICCMC). IEEE, 2019: 1018-1022.

[36] Tuli S, Tuli S, Tuli R, et al. Predicting the growth and trend of COVID-19 pandemic using machine learning and cloud computing[J]. Internet of Things, 2020, 11: 100222.

[37] Bibi N, Sikandar M, Ud Din I, et al. IoMT-based automated detection and classification of leukemia using deep learning[J]. Journal of Healthcare Engineering, 2020, 2020.

[38] Jia P , Wang X , Zheng K . Distributed Clock Synchronization Based on Intelligent Clustering in Local Area Industrial IoT Systems[J]. IEEE Transactions on Industrial Informatics, 2020, 16(6):3697-3707.

[39] Zhang C , Zhou G , Li H , et al. Manufacturing Blockchain of Things for the Configuration of a Data-and Knowledge-Driven Digital Twin Manufacturing Cell[J]. IEEE Internet of Things Journal, 2020, PP(99):1-1.

[40] Corral-Acero J , Margara F , Marciniak M , et al. The 'Digital Twin' to enable the vision of precision cardiology[J]. European Heart Journal, 2020.

[41] Croatti A, Gabellini M, Montagna S, et al. On the Integration of Agents and Digital Twins in Healthcare[J]. Journal of Medical Systems, 2020, 44(9): 1-8.

[42] Liu Y, Zhang L, Yang Y, et al. A novel cloud-based framework for the elderly healthcare services using digital twin[J]. IEEE Access, 2019, 7: 49088-49101.

[43] Gao Y, Tan K, Sun J, et al. Application of mixed reality technology in visualization of medical operations[J]. Chinese Medical Sciences Journal, 2019, 34(2): 103-109.

[44] Hamacher A, Kim S J, Cho S T, et al. Application of virtual, augmented, and mixed reality to urology[J]. International neurourology journal, 2016, 20(3): 172.

[45] Verhey J T, Haglin J M, Verhey E M, et al. Virtual, augmented, and mixed reality applications in orthopedic surgery[J]. The International Journal of Medical Robotics and Computer Assisted Surgery, 2020, 16(2): e2067.

[46] Gahlot S, Reddy S R N, Kumar D. Review of smart health monitoring approaches with survey analysis and proposed framework[J]. IEEE Internet of Things Journal, 2018, 6(2): 2116-2127.

[47] El Saddik A. Digital twins: The convergence of multimedia technologies[J]. IEEE multimedia, 2018, 25(2): 87-92.

[48] F. Biessmann, D. Salinas, S. Schelter, P. Schmidt, and D. Lange, "Deep learning for missing value imputation in tables with non-numerical data," Int. Conf. Inf. Knowl. Manag. Proc., pp. 2017–2026, 2018, doi: 10.1145/3269206.3272005.

[49] T. Kaneko, Y. Ushiku, and T. Harada, "Label-noise robust generative adversarial networks," Proc. IEEE Comput. Soc. Conf. Comput. Vis. Pattern Recognit., vol. 2019-June, no. 2, pp. 2462–2471, 2019, doi: 10.1109/CVPR.2019.00257.

[50] Xia X, Togneri R, Sohel F, et al. Auxiliary classifier generative adversarial network with soft labels in imbalanced acoustic event detection[J]. IEEE Transactions on Multimedia, 2018, 21(6): 1359-1371.

[51] M. D. Reid and R. C. Williamson, "Composite binary losses," J. Mach. Learn. Res., vol. 11, pp. 2387–2422, 2010.

[52] A. Dhurandhar et al., "Explanations based on the Missing: Towards contrastive explanations with pertinent negatives," in Advances in Neural Information Processing Systems, 2018, vol. 2018-Decem, no. NeurIPS, pp. 592–603.

[53] H. Zou and T. Hastie, "Regularization and variable selection via the elastic net," J. R. Stat. Soc. Ser. B Stat. Methodol., vol. 67, no. 2, pp. 301–320, 2005, doi: 10.1111/j.1467-9868.2005.00503.x.

[54] Wang X, Gao S, Wang M, et al. A Marching cube algorithm based on edge growth[J]. arXiv preprint arXiv:2101.00631, 2021.

[55] H. of cancer: the next generation., "A systematic review of data mining and machine learning for air pollution epidemiology," Cell, vol. 144, pp. 646–74, 3 2017.

[56] A. B. Parsa, A. Movahedi, H. Taghipour, S. Derrible, and A. Mohammadian, "Toward safer highways, application of xgboost and shap for real-time accident detection and feature analysis." Accident Analysis Prevention, vol. 136, p. 105405, 2020.

[57] P. Rajpurkar, J. Irvin, K. Zhu, B. Yang, H. Mehta, T. Duan, D. Ding, A. Bagul, C. Langlotz, and K. Shpanskaya, "Chexnet: Radiologist-level pneumonia detection on chest x-rays with deep learning," 2017.